Published in final edited form as:

Nat Neurosci. 2009 April ; 12(4): 399–408. doi:10.1038/nn.2294.

miR-124 regulates adult neurogenesis in the SVZ stem cell niche

Li-Chun Cheng[1], **Erika Pastrana**[1], **Masoud Tavazoie**[2], and **Fiona Doetsch**[1,2,3,4,§]

[1]Department of Pathology and Cell Biology, Columbia University, College of Physician and Surgeons, 630 West 168th Street, New York 10032

[2]Department of Neuroscience, Columbia University, College of Physician and Surgeons, 630 West 168th Street, New York 10032

[3]Department of Neurology, Columbia University, College of Physician and Surgeons, 630 West 168th Street, New York 10032

[4]Center for Motor Neuron Biology and Disease, Columbia University, College of Physician and Surgeons, 630 West 168th Street, New York 10032

Abstract

The subventricular zone (SVZ) is the largest neurogenic niche in the adult mammalian brain. Here we show that the brain-enriched microRNA miR-124 is an important regulator of the temporal progression of adult neurogenesis in mice. Knockdown of endogenous miR-124 maintains purified SVZ stem cells as dividing precursors, whereas ectopic expression leads to precocious and increased neuron formation. Furthermore, blocking miR-124 function during regeneration leads to hyperplasias followed by a delayed burst of neurogenesis. We identify the SRY-box transcription factor Sox9 to be a physiological target of miR-124 at the transition from transit amplifying cell to neuroblast stage. Sox9 over-expression abolishes neuronal differentiation whereas Sox9 knockdown leads to increased neuron formation. Thus, miR-124 mediated repression of Sox9 is important for progression along the SVZ stem cell lineage to neurons.

Introduction

The subventricular zone (SVZ) is the largest germinal region in the adult mammalian brain and harbours stem cells that generate olfactory bulb interneurons. The neural stem cells within this neurogenic niche are specialized astrocytes (Type B cells) that give rise to rapidly dividing transit amplifying cells (Type C cells) 1. The majority of these cells then

§Corresponding author, Fiona Doetsch, Ph: (212) 342-5633, Fax: (212) 305-5498 fkd2101@columbia.edu.

Author contributions

L.C. and F.D. initiated the project. L.C. generated pSR-GFP, pSR-124mt and pSR-shRNA constructs. L.C. and M.T. generated pSR-124. M.T. and E.P. generated pQC-Sox9. L.C. performed the *in situ* hybridization, qRT-PCR, neurosphere assays, neuron survival assays, Sox9 expression assay, retroviral production, penetratin conjugation, *in vivo* delivery and Ara-C experiments. L.C. and E.P. performed the FACS sorting, co-cultures, adherent cultures and *in vivo* injections. E.P. performed the Gene Ontology studies. M.T. performed the luciferase assays and Sox9 immunohistochemistry. F.D. was involved in study design, data collection, quantification and data analysis. The manuscript was written by F.D., L.C. and E.P. All authors performed data quantification, discussed the results and commented on the manuscript.

Note: Supplementary information is available on the Nature Neuroscience website.

generate neuroblasts (Type A cells) that migrate along the rostral migratory stream (RMS) and differentiate into granule and periglomerular interneurons in the olfactory bulb 1. A small number of oligodendrocytes are also generated by the adult SVZ 2, 3. Although much has been elucidated about the identity and lineage of SVZ stem cells, the regulatory mechanisms underlying *in vivo* stem cell self-renewal and differentiation are still largely unknown.

MicroRNAs (miRNAs) are small non-coding RNAs that are emerging as key post-transcriptional regulators implicated in developmental and disease processes 4, 5. miRNAs largely act as repressors of gene expression either by guiding the cleavage of their target mRNAs or by inhibiting their translation 4, 6. Their ability to potentially regulate large numbers of target genes simultaneously suggests that they may be important sculptors of transcriptional networks. As such, they are attractive candidates to regulate stem cell lineage progression. We have identified several miRNAs expressed at different stages of the SVZ stem cell lineage, one of which is miR-124, the most abundant miRNA in the adult brain 7. We therefore investigated the role of miR-124 in the adult SVZ neurogenic niche.

Previous work has shown that over-expression of miR-124 in HeLa cells shifts their mRNA profile towards a brain enriched pattern 8, whereas blocking miR-124 in cultured neurons leads to the up-regulation of non-neuronal transcripts 9. Based on *in vitro* over-expression in cell lines and in embryonic stem cells, miR-124 has been proposed to mediate neuronal differentiation 10, 11. This is achieved in part via targeting PTBP1, a repressor of neuron-specific splicing 11 and SCP1, a component of the REST transcription repressor complex 12. However, probing the role of miR-124 *in vivo* has been challenging. Two studies in the developing chick spinal cord investigating the role of miR-124 had differing findings. One reported that miR-124 has no effect on neuronal differentiation 13 whereas the other reported that miR-124 has modest effects on promoting neurogenesis 12. Thus, the *in vivo* role of miR-124 in neurogenesis is still unclear.

Here we uncover a novel role for miR-124 in regulating the temporal progression of neurogenesis in the adult SVZ. miR-124 is first up-regulated at the transition between transit amplifying cells and neuroblasts, and further increases as neuroblasts exit the cell cycle. Blocking miR-124 maintains SVZ cells as dividing precursors, whereas ectopic expression of miR-124 promotes precocious neuronal differentiation. Knockdown of endogenous miR-124 during regeneration leads to the formation of hyperplasias and a delay in neuronal regeneration. We identify *dlx-2, jagged-1* and *sox9* as miR-124 targets. We show that *sox9* is an important physiological target of miR-124 in SVZ neuroblasts where *sox9* mRNA is present but not protein. Sox9 over-expression in SVZ cells abolishes the production of neurons. In contrast, Sox9 knockdown leads to increased neurogenesis and decreased glial formation. Thus, the protein levels of Sox9 must be down-regulated for neuronal differentiation and are tightly controlled at the post-transcriptional level by miR-124 as cells progress along the SVZ lineage.

Results

miR-124 is expressed by neuroblasts in the adult SVZ niche

To determine the spatial and cell-type specific distribution of miR-124 in the adult SVZ neural stem cell niche, we performed *in situ* hybridization using DIG-labeled RNA probes targeting the mature form of miR-124. miR-124 was expressed at low levels in both the SVZ and RMS (Fig. 1a–d) and was greatly up-regulated in mature granule and periglomerular neurons in the olfactory bulb (Fig. 1b, e) at levels seen in mature neurons throughout the brain (Fig. 1h, Supplementary Fig. 1a). In contrast, miR-124 was not expressed in oligodendrocytes or astrocytes (data not shown). To distinguish which cell types in the adult SVZ express miR-124, we performed *in situ* hybridization in combination with immunostaining for markers expressed at different stages of the SVZ lineage (Fig. 1f). miR-124 was not expressed at the earliest stages of the lineage in brain lipid binding protein ($BLBP^+$) SVZ astrocytes or in dividing doublecortin-negative (DCX^-) transit amplifying cells (Fig. 1g, h) but was expressed in DCX^+ neuroblasts (Fig. 1g, h). Interestingly, miR-124 was expressed in a similar pattern in germinal zones in the developing forebrain. miR-124 was largely absent in the ventricular zone (VZ) at E11, E14 and E17, with the exception of a few individual cells at E11 and E14 (Supplementary Fig. 1b–g), which likely correspond to the first appearing neurons 14, 15. At E14 and E17, miR-124 was highly expressed in the SVZ (Supplementary Fig. 1d, f) and was present at high levels in the cortical plate at E17 (Supplementary Fig. 1f).

To confirm our *in situ* hybridization expression results we used another approach to detect miRNAs in the adult SVZ. We have recently developed a simple strategy to prospectively isolate cells at each stage of the SVZ stem cell lineage using fluorescence activated cell sorting (FACS) based on the differential expression of glial fibrillary acidic protein (GFAP), epidermal growth factor receptor (EGFR) and mCD24 16 (Fig. 1f). This approach makes use of the fact that activated stem cells express the EGFR, as do transit amplifying cells 17. By sorting from *GFAP-GFP* mice, in which SVZ astrocytes express GFP, stem cell astrocytes ($EGFR^+$) can be separated from niche astrocytes ($EGFR^-$) based on binding to a fluorescently complexed EGF-ligand. By combining these two markers with mCD24, which labels neuroblasts and ependymal cells with different intensities but not astrocytes and transit amplifying cells, SVZ stem cell astrocytes ($GFAP^+EGFR^+mCD24^-$), transit amplifying cells ($GFAP^-EGFR^+mCD24^-$) and neuroblasts ($GFAP^-EGFR^-mCD24^{low}$) can all be isolated in a single sort 16.

We therefore performed quantitative RT-PCR (qRT-PCR) for miR-124 on FACS purified SVZ cells. As seen by *in situ* hybridization, qRT-PCR confirmed that miR-124 was highly expressed in neuroblasts as compared to other SVZ cell types (Fig. 1i). In addition, by using the DNA dye (Vybrant DyeCycle) to separate neuroblasts at different stages of the cell cycle 16, we found that miR-124 levels were higher in neuroblasts in G0/G1 phase as compared to S/G2-M phase (Fig. 1i). Thus, miR-124 is up-regulated as cells transition from transit amplifying cells to neuroblasts, and further increases as neuroblasts exit the cell cycle.

miR-124 knockdown retains SVZ cells as dividing precursors

The above expression analysis suggests that miR-124 is important for lineage progression during adult neurogenesis. To determine the functional role of miR-124, we performed knockdown studies on FACS purified SVZ cell populations. Mouse SVZ stem cell astrocytes were plated at clonal density on neonatal (P0) rat cortical astrocytes in a co-culture assay 18, 19. We identified the progeny of plated SVZ cells using mouse specific M2/M6 antibodies 19. To assess proliferation, BrdU was added during the final 24 hours of culture. After 5 days *in vitro*, colonies containing postmitotic neurons ($TuJ1^+BrdU^-$), dividing neuroblasts ($BrdU^+TuJ1^+$), dividing precursors ($BrdU^+TuJ1^-$) and M2/M6 only cells were present (Fig. 2a). The majority of M2/M6 only cells had a typical astrocytic morphology (Fig. 2a); we did not detect $O4^+$ oligodendrocytes in this co-culture assay (data not shown), presumably due to the pro-neurogenic environment created by neonatal astrocytes 18.

To block miR-124 function, cultures were treated with penetratin (pen)-conjugated 2'-O-methyl (2'OMe) antisense miR-124 (AS-124) 20–22, which is efficiently taken up by SVZ cells (Supplementary Fig. 2a) and knocks down endogenous miR-124 (Supplementary Fig. 2b). As a control we used 2'OMe antisense RNA against miR-194 (AS-194) (Supplementary Fig. 2c), a microRNA enriched in liver and kidney 23. miR-124 knockdown resulted in a ~30% decrease in the total number of post-mitotic neurons and an increase in the total number of dividing cells (1.7-fold to untreated culture and 1.3-fold to AS-194 treated culture (Fig. 2a–d). Analysis of individual colonies revealed that blocking miR-124 led to an increase of both dividing neuroblasts ($TuJ1^+BrdU^+$) and transit amplifying cells ($TuJ1^-BrdU^+$) (Fig. 2e).

Blocking miR-124 caused an overall increase in the total number of cells (Supplementary Fig. 2d) not only by retaining SVZ cells as dividing precursors within each colony but also by increasing the total number of colonies formed in the co-culture (Supplementary Fig. 2e). This could be due to blocking the progression of precursors along the lineage at the transit amplifying stage. Alternatively, miR-124 knockdown may revert differentiating neuroblasts back to an EGF responsive state. We therefore used the neurosphere assay to directly address this question, as both stem cell astrocytes and transit amplifying cells generate neurospheres but neuroblasts do not 16, 17.

The number of neurospheres formed from unpurified SVZ cells treated with AS-124 increased 1.3 fold and 1.5 fold as compared to penetratin-only and AS-194 treated cultures respectively (Fig. 2f). To identify which SVZ cell types were being affected by miR-124 knockdown, the neurosphere forming capacity of FACS-sorted populations from each stage of the lineage was compared after culture with AS-124. Only the number of neurospheres formed by transit amplifying cells was significantly increased by miR-124 knockdown (Fig. 2f). Importantly, no neurospheres formed in AS-124 treated purified neuroblasts (Fig. 2f) showing that AS-124 treatment is not causing neuroblasts to revert back to an EGF-responsive state.

Furthermore, miR-124 knockdown in purified neuroblasts did not affect survival (Fig. 2g) or their capacity to mature and extend neurites when cultured on laminin (Supplementary Fig.

3) with continuous AS-124 treatment for 5 days. Thus, the onset of miR-124 expression as SVZ cells transition from transit amplifying cells to neuroblasts is important for SVZ cells to proceed from an actively proliferating state into differentiating neuroblasts in the SVZ stem cell lineage.

miR-124 over-expression promotes neuronal differentiation

To examine the consequences of ectopically expressing miR-124 at earlier stages in the SVZ lineage, we generated a replication incompetent retrovirus (RV-124) that encodes dual promoters driving the expression of miR-124 and GFP (Fig. 3a). Importantly, this retroviral construct produces physiological levels of miR-124 comparable to those expressed by G0/G1 SVZ neuroblasts (Fig. 3c). As a control, we mutated six nucleotides in the seed region at the 5' end of miR-124 (miR-124mt) (Fig. 3b) to disrupt its interaction with miR-124 targets.

In contrast to miR-124 knockdown, which maintained SVZ cells as dividing precursors at the expense of neuron formation, miR-124 over-expression had the opposite effect. MiR-124 over-expression caused a significant decrease in the overall proportion of dividing cells and an increase in postmitotic neurons (Fig. 3d, e). Analysis of individual colonies revealed that RV-124 transduced cells generated smaller colonies than RV-GFP transduced cells (Supplementary Fig. 4). Frequently the colonies comprised only one or two post-mitotic $TuJ1^+$ neurons suggesting that miR-124 over-expression causes cell cycle exit. In addition, miR-124 over-expression also caused a significant decrease in astrocytic cells ("other" cells) (Fig. 3d, e).

miR-124 regulates neurogenesis in the SVZ stem cell niche

To define the function of miR-124 *in vivo*, we analyzed the effect of miR-124 knockdown and over-expression on SVZ lineage progression under homeostasis. RV-GFP, RV-124mt or RV-124 were stereotactically injected into the SVZ of adult mice to infect dividing precursors. To block miR-124 *in vivo*, a mini-osmotic pump filled with AS-124 was implanted into the lateral ventricle immediately after RV-GFP injection. Three days after RV injection, whole mounts were dissected and the lineage progression of GFP labeled cells analyzed. Both GFP^+ post-mitotic neurons in migratory chains and clusters of dividing cells were present in the SVZ (Fig. 4a, e).

In vivo knockdown of miR-124 resulted in an ~30% decrease in post-mitotic neurons accompanied by an ~1.5 fold increase in dividing cells (Fig. 4b–d). Conversely, over-expression of miR-124 by RV-124 resulted in an ~1.3 fold increase in the proportion of post-mitotic neurons and a decrease in dividing precursors (Fig. 4f–h). Two weeks after infection, labeled neurons were present in the granule and periglomerular cell layers of the olfactory bulb (Supplementary Fig. 5a), suggesting that miR-124 over-expression does not affect neuronal migration. Consistent with the above *in vitro* findings, miR-124 over-expression also led to a significant decrease in astrocyte-like cells *in vivo*. However ectopic expression of physiological levels of miR-124 does not appear to impair the production of Olig2 positive oligodendrocyte lineage cells (Supplementary Fig. 5b, c).

Blocking endogenous miR-124 delays neuronal regeneration

The adult SVZ rapidly regenerates after anti-mitotic treatment. When the SVZ is depleted of transit amplifying cells and neuroblasts using cytosine-β-D-arabinofuranoside (Ara-C), SVZ stem cells astrocytes that do not divide during Ara-C treatment proliferate and regenerate the network of chains of neuroblasts via transit amplifying cells (Fig. 5a–c) 1, 24. Differentiating neurons first appear in foci after 4.5–5 days of regeneration (Fig. 5d, e), and they form migratory chains around 6.5–7 days (Fig. 5l, m). Because regeneration only takes about one week, it is feasible to block miR-124 throughout and directly ask whether miR-124 is required for neuronal differentiation itself or whether it regulates the timing of progression along the SVZ lineage. We infused Ara-C for 6 days to eliminate transit amplifying cells and neuroblasts. After Ara-C treatment, we implanted a pump containing either penetratin-alone or AS-124 into the lateral ventricle for 5 days or 7 days (Fig. 5a).

Strikingly, neuroblast foci were almost completely absent after 5 days of miR-124 knockdown. Very few $TuJ1^+$ (Fig. 5h) or DCX^+ (Fig. 5i) cells were present in whole mounts of AS-124 treated brains. In contrast the number of $Ki67^+$ cells increased two-fold (AS-124, 2852 cells/mm^2 vs saline, 1347 cells/mm^2 ($p=0.0089$, Newman-Keuls test), vs penetratin only, 1686 cells/mm^2 ($p=0.0135$, Newman-Keuls test)). Intriguingly, hyperplasias of dividing cells occurred frequently in the SVZ suggesting that SVZ precursors failed to differentiate into neuroblasts and were retained as transit amplifying cells (Fig. 5g). After 7 days of regeneration with AS-124 treatment, the proliferating SVZ precursors differentiated *en masse* into neuroblasts and formed large disorganized clusters (Fig. 5p, q) that disrupted the migratory chains present in control brains (Fig. 5l, m). Thus knocking down endogenous miR-124 delays regeneration but does not permanently block neuronal differentiation.

Together, the loss and gain of function analyses, both *in vitro* and *in vivo* under homeostasis and during regeneration, reveal that miR-124 is a key regulator of the timing of SVZ lineage progression at the transition from transit amplifying cells to neuroblasts.

Sox9 is a direct target of miR-124 in the SVZ lineage

Individual miRNAs can regulate numerous target mRNAs at the post-transcriptional level 4. To identify potential physiological targets of miR-124 in the SVZ, we performed a Gene Ontology analysis of its computationally predicted targets from TargetScan 25. Analysis of over-representation of gene classes among miR-124 targets compared to the mouse genome highlighted “development” and “cell differentiation” as significantly enriched GO groups (Supplementary Table 1). We cross-compared miR-124 targets to those of heart-enriched miR-1 26, B cell-enriched miR-181 27, miR-194 23 and another brain-enriched miRNA miR-9 28. Among miR-124 targets, “cell differentiation” genes were consistently highlighted across all comparisons (Supplementary Table 2).

Among the predicted “cell differentiation” targets were several known to be expressed in the SVZ and involved in the progression of the SVZ stem cell lineage. These include *dlx2*, a transcription factor involved in interneuron formation 17, 29 and the Notch ligand *jagged1*, which is important for self-renewal in the SVZ 30. Intriguingly, *sox9*, an SRY-box transcription factor which has been implicated in glial cell specification during development

31, 32 and stem cell maintenance in the intestinal epithelium and hair follicle 33–35 was also a predicted target. Unlike, *dlx2* and *jagged1*, the role of *sox9* in the adult SVZ is unknown. We validated these three gene candidates as miR-124 targets by performing luciferase assays (Fig. 6a). The 3'UTRs of *dlx2*,*jagged1* and *sox9* were cloned into luciferase reporter vectors (Fig. 6b) and co-transfected with miR-124 into HeLa cells. miR-124 significantly decreased luciferase activity in all three constructs, with the largest effect observed for *sox9* (Fig. 6a).

Given the glial identity of stem cells in the adult brain, progression along the SVZ lineage into neurons requires that glial genes as well as those involved in self-renewal be down-regulated. As such, *sox9* is an attractive miR-124 target. miR-124 over-expression dramatically reduced Sox9 protein levels in neonatal cortical astrocytes (Fig. 6c–f) and adult SVZ cells cultured as adherent cells with EGF (Fig. 6g–i), both of which express high levels of Sox9.

To investigate whether *sox9* is an *in vivo* physiological target of miR-124 in the adult SVZ, the expression patterns of Sox9 protein and mRNA were analyzed by immunohistochemistry (Fig. 6j–m) and *in situ* hybridization (Fig. 6n–p). Sox9 protein was present in ependymal cells and was expressed by all SVZ astrocytes and approximately 30% of transit amplifying cells, but not by neuroblasts (Fig. 6j–m). Interestingly, although neuroblasts did not express Sox9 protein, they had detectable levels of *sox9* mRNA (Fig. 6n–p), suggesting that Sox9 is post-transcriptionally regulated by miR-124 *in vivo*. Indeed, knockdown of endogenous miR-124 with AS-124 resulted in up-regulation of Sox9 protein in dividing neuroblasts both *in vitro* (Fig. 7a, b) and *in vivo* in migratory chains (Fig. 7c–e). Thus miR-124 regulates endogenous Sox9 expression in the adult SVZ.

Sox9 protein is also expressed in neural stem cells in the VZ of the developing brain (Supplementary Fig. 6a–d). Interestingly, the onset of Sox9 in the forebrain parallels that of miR-124 but they are spatially exclusive (Supplementary Fig. 6e–h). Therefore, it is very likely that Sox9 is under similar post-transcriptional control mediated by miR-124 in neurogenesis during development.

Sox9 down-regulation is required for neurogenesis

The *in vivo* expression pattern of Sox9 shows that it is down-regulated during neurogenesis. To evaluate the effect of Sox9 over-expression, we generated a replication incompetent retrovirus encoding only the open reading frame of *sox9* (RV-Sox9) and lacking the 3'UTR, which has two miR-124 target sites (Fig. 8a). miR-124 over-expression in SVZ adherent cultures led to a two-fold increase in the number of neurons and a one third reduction in the number of $GFAP^+$ astrocytes generated (Fig. 8b, c, h). In contrast, Sox9 over-expression maintained SVZ cells as $GFAP^+$ astrocytes and completely eliminated neuronal production (Fig. 8d, h). Simultaneous miR-124 over-expression did not rescue neuronal production in Sox9 over-expressing cells (Fig. 8e, h). Neither miR-124 nor Sox9 over-expression affected oligodendrocyte formation. However, this may be due to the low number of oligodendrocytes generated (data not shown).

Conversely, to investigate the effect of Sox9 knockdown on differentiation, two shRNAs targeting sox9 transcripts were cloned into the MSCV retroviral vector. shSox9-C was more potent at knocking down endogeous Sox9 and decreased Sox9 protein levels 5-fold (Supplementary Fig. 7a, c–e), . In contrast, shSox9-A only mildly decreased Sox9 levels (Supplementary Fig. 7b, d, e).

Knockdown of Sox9 by RV-shSox9-C significantly increased the proportion of neurons generated mimicking the effect induced by RV-124 (Fig. 8b, f, g, i). These results suggest that *sox9* is a key target of miR-124 in neuronal differentiation. No significant effect was observed with either RV-Sox9-A or RV-Sox9-C on the production of $GFAP^+$ astrocytes (Fig. 8i) suggesting that low levels of Sox9 expression are sufficient for maintaining astrocyte differentiation.

Thus, these functional experiments reveal that Sox9 transcripts interact with miR-124 at the transition of SVZ transit amplifying cells to neuroblasts and that down-regulation of Sox9 permits neuronal differentiation. Altogether, the results suggest that Sox9 protein levels need to be tightly controlled within the SVZ lineage and that post-transcriptional regulation of Sox9 by miR-124 is a key step in the glial-to-neuron transition along the SVZ stem cell lineage.

Discussion

In this study we show for the first time that miRNAs are important regulators of adult neurogenesis *in vivo* in the SVZ stem cell niche. We find that the brain-enriched miRNA, miR-124, is differentially expressed in neuroblasts in the stem cell lineage, with levels increasing as they exit the cell cycle. Under both homeostasis and regeneration, miR-124 functionally regulates the timing of the transition between transit amplifying cells and neuroblasts by promoting neuronal differentiation and cell cycle exit and repressing genes important for stem cell self-renewal and glial differentiation (see model in Supplementary Fig. 8). Moreover, post-transcriptional regulation of Sox9 by miR-124 is a critical step that allows glial stem cells to transition into neurons in adult neurogenesis.

MiR-124 was one of the first miRNAs identified in mammals due to its abundant expression in the mature brain 7. Its temporal expression profile suggested that it may play a role in both brain development and in mature neuronal function 10, 36. As previously reported 28, we observed miR-124 expression in mature neurons, and not in glial cells. The first evidence that miR-124 may be implicated in neuronal differentiation came from P19 carcinoma cells and ES cells 10, 11. miR-124 may act in part by silencing REST, a transcriptional repressor of neuronal gene expression 9, 12, and switching on neuron-specific splicing by targeting PTBP1, a repressor of pre-mRNA splicing in non-neuronal cells 11. However, the *in vivo* function of miR-124 is unclear. One study in the developing chick spinal cord reported that blocking miR-124 has no effect on neurogenesis, whereas another suggested that miR-124 has a modest role in neuronal differentiation and cell cycle exit 12, 13. The discrepancy between these results may be technical, as transient transfection of antisense oligonucleotides may not be sufficient to knockdown miR-124 levels as progenitor cells proliferate frequently and may dilute their efficacy. Furthermore, electroporation was used

to introduce high levels of either miR-124 duplexes or precursors, which may overwhelm the capacity of the endogenous miRNA processing machinery to produce the normal complement of miRNAs, and possibly cause off-target effects.

Here we identify at single cell resolution which cells express miR-124 *in vivo* in the adult SVZ, and quantitatively analyze miR-124 expression levels in FACS purified populations. These approaches have revealed that miR-124 acts at the transition from transit amplifying cells to neuroblasts. By manipulating physiological levels of miR-124 in purified SVZ cells *in vitro*, as well as *in vivo*, both under homeostasis and regeneration, we have defined the function of miR-124 in adult neurogenesis. We find, in agreement with a previous study in the developing spinal cord 12, that miR-124 promotes neuronal differentiation and cell cycle exit in the adult SVZ. Our observations further suggest that miR-124 is not involved in neuronal versus glial cell fate decisions. Loss of miR-124 in SVZ cells is not sufficient to cause gliogenesis, likely because neuron/glial fate decisions are made by other factors prior to endogenous miR-124 expression *in vivo*. Importantly, we uncover a novel role for miR-124, namely the regulation of timing of neuronal differentiation along the SVZ stem cell lineage. This is most clearly seen during regeneration, where blocking miR-124 led to a temporary arrest at the transit amplifying stage and the formation of hyperplasias, followed by a delayed burst of neuronal production. As such, we propose that miR-124 is a key player in the temporal regulation of progression along the SVZ stem cell lineage.

Stem cells in the adult SVZ are a subset of astrocytes. As such, progression along the SVZ lineage into neurons requires the down-regulation of genes involved in glial function and self-renewal. Consistent with this, miR-124 over-expression reduced the number of astrocytes formed. Here we have focused on the transcription factor *sox9* as a physiological target of miR-124. Sox9 regulates glial fate specification and controls the transcription of glial gene networks in the central nervous system31, 32 as well as self-renewal in other stem cell niches. We validated *sox9* to be a bona fide miR-124 target and show that Sox9 protein levels can be directly controlled by miR-124 through its 3'UTR. Interestingly, *sox9* transcripts are present in neuroblasts, and co-exist with miR-124 both spatially and temporally. Furthermore, when we blocked endogenous miR-124, Sox9 protein was up-regulated in neuroblasts, which are still in cell cycle. Thus Sox9 levels are regulated in neuroblasts post-transcriptionally by miR-124. It will be intriguing to determine whether Sox9 directly regulates the cell cycle. Our data further suggest that the down-regulation of Sox9 is necessary for neuronal differentiation. *In vivo*, Sox9 levels decrease as cells progress along the SVZ lineage and Sox9 knockdown in SVZ adherent cultures led to an increase in the number of neurons formed. As Sox9 is expressed in multiple SVZ cell types, including stem cells and transit amplifying cells, conditional knockout of Sox9 in a cell type specific manner will be required to dissect its role *in vivo* in stem cell self-renewal, proliferation and in gliogenesis.

Two models of miRNA repression of target genes have been proposed: (1) complete elimination of protein expression and (2) balancing target protein levels 37. Most reported miR-124 targets, including *scp1*12, *ptbp1*11 and *lamc1*13, as well as *sox9* and *jagged1*, two targets we describe here, show reciprocal protein expression with miR-124 suggesting that miR-124 keeps these genes silenced. In contrast, miR-124 and Dlx-2 protein are

simultaneously expressed in SVZ neuroblasts, with Dlx-2 levels lower than in transit amplifying cells 17. This suggests that miR-124 balances Dlx-2 translation to a defined level as cells differentiate.

The expression of miR-124 is thought to be regulated by REST 9. This zinc-finger repressor negatively regulates many neuronal genes in stem cells, progenitors and non-neuronal cell types 38. Potential REST binding sites are located near all three *mir-124* loci 9, and miR-124 up-regulation is likely a result of de-repression of the REST repressor complex during neuronal differentiation. Indeed, miR-124 expression is up-regulated in $REST^{+/-}$ embryonic stem cell lines 9, 39. One component of the REST repressor complex, SCP1, is among miR-124 targets and is expressed in the VZ germinal region in the developing spinal cord 12. By targeting SCP1, miR-124 may reinforce its own expression in neurons through repressing REST activity.

It is important to note that miR-124 continues to be expressed by mature neurons throughout the brain, suggesting that miR-124 likely has other physiological functions in mature neurons, in addition to its functional role in neurogenesis.

Conclusion

Here we provide the first evidence that miRNAs regulate adult neural stem cell lineages *in vivo*. It will be important to define the full complement of miRNAs expressed at each stage in the SVZ lineage to uncover their regulatory networks and compare them to those involved in other neuronal systems 40. miR-124 plays an important role in maintaining SVZ homeostasis, by regulating the number of progenitors and the timing of neuronal differentiation. Understanding the pleiotropic effects mediated by miR-124 may uncover novel approaches towards stimulating neurogenesis in non-neurogenic brain areas, and in inhibiting the progression of brain tumours 41.

Methods

All animal care was in accordance with institutional guidelines and IACUC approval. Detailed procedures for immunostaining, FACS, cell culture, retroviral constructs, luciferase reporter assays, and western blots are described in the Supplementary Methods online.

In situ hybridization

miRNA probes were generated with the *mirVana* probe construction kit (Ambion). For detecting *sox9*, I.M.A.G.E. clone ID# 3666566 was used. *In vitro* transcription of digoxigenin-labeled RNA probes was performed according to manufacturer's protocols. Embryonic brains from stages E11, E14 and E17 and 2 month old CD-1 mice (Charles River Lab) were perfused with 3% paraformaldehyde (PFA)/0.1% glutaraldehyde (for miRNA) or with 3% PFA (for *sox9*). Brains were immersed in 30% sucrose, embedded in Tissue-Tek OCT, and sectioned on the cryostat. 12 μm coronal or 25 μm sagittal sections were acetylated and hybridized with digoxygenin-labeled (DIG) RNA probes overnight at 42 °C (miRNA) or at 68 °C (*sox9*). Sections were washed extensively and treated with RNase after

hybridization. Signals were revealed using alkaline phosphatase conjugated anti-digoxygenin antibodies (1:4000, Roche) and NBT/BCIP.

Fluorescence activated cell sorting

The different cell stages of the SVZ lineage were purified following procedures described in 16. Detailed procedures are described in the Supplementary Methods.

RNA extraction and quantitative reverse transcription PCR

For qRT-PCR of miRNA, the small RNA fraction was isolated with *mirVana* miRNA isolation kit (Ambion) and 250 pg were used for each reaction. qRT-PCR was performed in triplicates using SYBR green on a Stratagene MX3000 thermocycler (Stratagene). The Ct value is determined using automatic baseline determination feature on Stratagene MX3000 and the relative expression of miR-124 was normalized to 5S rRNA using $2^{-\Delta Ct}$ equation.

Penetratin-1 mediated delivery

Antisense 2'-O-methyl RNA oligonucleotides (2'OMe-RNAs) containing a 5'-thiol group (Dharmacon) were conjugated to Penetratin-1 (Qbiogene) as described 22.

Co-cultures

Co-cultures were based on previously described protocols 19, 42 and adapted to FACS purified SVZ populations. Detailed procedures are described in the Supplementary Methods.

Neurosphere assays

Neurosphere assays were performed from FACS purified SVZ populations as described 17.

Neuron survival assays

FACS purified SVZ neuroblasts ($CD24^{low}$ population) were plated at 20,000 cells per cm^2 on 16-well LabTek chamber slides coated with 0.5 mg/ml PDK (Sigma) and 0.01 mg/ml Laminin (Sigma). Cells were cultured for 5 days in NB/B27 with 200 nM penetratin1-conjugated antisense 2'OMe-RNAs. Cell Tracker (1 μM, Molecular Probes) was added to the cells for 30 minutes at 37 °C prior to fixation and staining.

Adherent cultures

Adult SVZ cells were dissociated and plated on 16-well LabTek chamber slides coated with 0.01 mg/ml Laminin at 10,000 cells per cm^2. Cells were grown in DMEM-F12 supplemented with N2, 2 mM glutamine, 20 μg/ml insulin, 15 mM HEPES and 20 ng/ml EGF.

Animal surgery

Retroviruses (0.2 μl with 8 μg/ml polybrene in solution) were stereotaxically injected into the two hemispheres of anaesthetized 2 month old CD-1 mice (coordinates relative to bregma: anterior (A), lateral (L), depth (D): 0, 1.4, 1.6; 0.5, 1.1, 1.7; 1, 1, 2.3). After three days, mice were perfused with saline and SVZ whole mounts were dissected, fixed and processed for immunostaining. To block miR-124 *in vivo*, 4 μM of penetratin-conjugated

2'OMe-RNAs in 100 μL saline were delivered by micro-osmotic pump (Model: 1007D, Durect) into the right ventricle (coordinates A, L, D: 0, 1, 2.6) directly after retroviral injection. Only cells in the right SVZ were quantified in the miR-124 knockdown experiment. For the regeneration assay, micro-osmotic pumps filled with 2% cytosine-β-D-arabinofuranoside (Ara-C, Sigma) were implanted onto the surface of the brain as previously described 24. After 6 days of Ara-C infusion, the implant was replaced with a second pump filled with penetratin-conjugated 2'OMe-RNAs for an additional 5 or 7 days.

Quantification and statistical analysis

Images were taken under the 20x objective of the inverted Axiovert200 microscope (Zeiss). Cells were quantified blind employing the ImageJ software. A minimum of 20 randomly chosen fields were quantified for the neuroblast survival, and adherent culture assays. In the co-culture experiments, we counted all the $M2M6^+$ or GFP^+ cells present in the wells. All experiments were done a minimum of three times. The mean ± s.e.m. values are represented in the histograms. Statistical comparison of datasets was performed by two-tailed paired Students-*t* test except if noted otherwise. The differences are presented with their corresponding statistical significance or *p* value.

Computational analysis of miR-124 targets

The Functional Annotation Clustering and the overrepresentation statistics of the predicted miR-124 targets (TargetScan) was performed by DAVID-EASE software (http://david.niaid.nih.gov/david/ease.htm). Potential miR-124 targets with highest EASE score (Cell Differentiation) were further confirmed with their expression pattern in Allen Brain Atlas (http://www.brain-map.org/welcome.do).

Supplementary Material

Refer to Web version on PubMed Central for supplementary material.

Acknowledgements

We thank Kristie Gordon for assistance with FACS at the Herbert Irving Comprehensive Cancer Center (HICCC) at Columbia University. We thank members of the Doetsch and Wichterle labs for critical reading of the manuscript. We are grateful to C. Troy for advice on penetratin-1 mediated delivery; N. Heintz for anti-BLBP antibody; J. Johnson for anti-Mash1 antibody; R. Tsien for pCMV-Cherry plasmid. The nestin, M2 and M6 antibodies developed by S. Hockfield and C. Lagenaur, respectively, were obtained from the Developmental Studies Hybridoma Bank developed under the auspices of the NICHD and maintained by The University of Iowa, Department of Biological Sciences. This work is supported by an NIH NINDS grant. E. P. was supported by an NIH training grant and a grant from the Spanish Ministerio de Educacion y Ciencia. M.T. is supported by a MSTP fellowship from the NIH, F. D. is a Packard Foundation Fellow and Irma T. Hirschl fellow and the work is partially supported by the Jerry and Emily Spiegel Laboratory for Cell Replacement Therapies and the Anne and Bernard Spitzer Fund for Cell Replacement Therapy.

References

1. Doetsch F, Caille I, Lim DA, Garcia-Verdugo JM, Alvarez-Buylla A. Subventricular zone astrocytes are neural stem cells in the adult mammalian brain. Cell. 1999; 97:703–716. [PubMed: 10380923]
2. Menn B, et al. Origin of oligodendrocytes in the subventricular zone of the adult brain. J Neurosci. 2006; 26:7907–7918. [PubMed: 16870736]

3. Lachapelle F, Avellana-Adalid V, Nait-Oumesmar B, Baron-Van Evercooren A. Fibroblast growth factor-2 (FGF-2) and platelet-derived growth factor AB (PDGF AB) promote adult SVZ-derived oligodendrogenesis in vivo. Mol Cell Neurosci. 2002; 20:390–403. [PubMed: 12139917]
4. Bartel DP. MicroRNAs: genomics, biogenesis, mechanism, and function. Cell. 2004; 116:281–297. [PubMed: 14744438]
5. Stefani G, Slack FJ. Small non-coding RNAs in animal development. Nat Rev Mol Cell Biol. 2008; 9:219–230. [PubMed: 18270516]
6. Flynt AS, Lai EC. Biological principles of microRNA-mediated regulation: shared themes amid diversity. Nat Rev Genet. 2008; 9:831–842. [PubMed: 18852696]
7. Lagos-Quintana M, et al. Identification of tissue-specific microRNAs from mouse. Curr Biol. 2002; 12:735–739. [PubMed: 12007417]
8. Lim LP, et al. Microarray analysis shows that some microRNAs downregulate large numbers of target mRNAs. Nature. 2005; 433:769–773. [PubMed: 15685193]
9. Conaco C, Otto S, Han JJ, Mandel G. Reciprocal actions of REST and a microRNA promote neuronal identity. Proceedings of the National Academy of Sciences of the United States of America. 2006; 103:2422–2427. [PubMed: 16461918]
10. Krichevsky AM, Sonntag KC, Isacson O, Kosik KS. Specific microRNAs modulate embryonic stem cell-derived neurogenesis. Stem Cells. 2006; 24:857–864. [PubMed: 16357340]
11. Makeyev EV, Zhang J, Carrasco MA, Maniatis T. The MicroRNA miR-124 promotes neuronal differentiation by triggering brain-specific alternative pre-mRNA splicing. Molecular Cell. 2007; 27:435–448. [PubMed: 17679093]
12. Visvanathan J, Lee S, Lee B, Lee JW, Lee SK. The microRNA miR-124 antagonizes the anti-neural REST/SCP1 pathway during embryonic CNS development. Genes & Development. 2007; 21:744–749. [PubMed: 17403776]
13. Cao X, Pfaff SL, Gage FH. A functional study of miR-124 in the developing neural tube. Genes & Development. 2007; 21:531–536. [PubMed: 17344415]
14. Noctor SC, Flint AC, Weissman TA, Dammerman RS, Kriegstein AR. Neurons derived from radial glial cells establish radial units in neocortex. Nature. 2001; 409:714–720. [PubMed: 11217860]
15. Haubensak W, Attardo A, Denk W, Huttner WB. Neurons arise in the basal neuroepithelium of the early mammalian telencephalon: a major site of neurogenesis. Proceedings of the National Academy of Sciences of the United States of America. 2004; 101:3196–3201. [PubMed: 14963232]
16. Pastrana E, Cheng L-C, Doetsch F. Simultaneous prospective purification of adult subventricular zone neural stem cells and their progeny. Proceedings of the National Academy of Sciences of the United States of America, in press. 2009
17. Doetsch F, Petreanu L, Caille I, Garcia-Verdugo JM, Alvarez-Buylla A. EGF converts transit-amplifying neurogenic precursors in the adult brain into multipotent stem cells. Neuron. 2002; 36:1021–1034. [PubMed: 12495619]
18. Lim DA, Alvarez-Buylla A. Interaction between astrocytes and adult subventricular zone precursors stimulates neurogenesis. Proceedings of the National Academy of Sciences of the United States of America. 1999; 96:7526–7531. [PubMed: 10377448]
19. Malatesta P, Hartfuss E, Gotz M. Isolation of radial glial cells by fluorescent-activated cell sorting reveals a neuronal lineage. Development. 2000; 127:5253–5263. [PubMed: 11076748]
20. Meister G, Landthaler M, Dorsett Y, Tuschl T. Sequence-specific inhibition of microRNA-and siRNA-induced RNA silencing. RNA. 2004; 10:544–550. [PubMed: 14970398]
21. Hutvagner G, Simard MJ, Mello CC, Zamore PD. Sequence-specific inhibition of small RNA function. PLoS Biology. 2004; 2:E98. [PubMed: 15024405]
22. Davidson TJ, et al. Highly efficient small interfering RNA delivery to primary mammalian neurons induces MicroRNA-like effects before mRNA degradation. J Neurosci. 2004; 24:10040–10046. [PubMed: 15537872]
23. Sempere LF, et al. Expression profiling of mammalian microRNAs uncovers a subset of brain-expressed microRNAs with possible roles in murine and human neuronal differentiation. Genome Biology. 2004; 5:R13. [PubMed: 15003116]

24. Doetsch F, Garcia-Verdugo JM, Alvarez-Buylla A. Regeneration of a germinal layer in the adult mammalian brain. Proceedings of the National Academy of Sciences of the United States of America. 1999; 96:11619–11624. [PubMed: 10500226]
25. Lewis BP, Shih IH, Jones-Rhoades MW, Bartel DP, Burge CB. Prediction of mammalian microRNA targets. Cell. 2003; 115:787–798. [PubMed: 14697198]
26. Zhao Y, Samal E, Srivastava D. Serum response factor regulates a muscle-specific microRNA that targets Hand2 during cardiogenesis. Nature. 2005; 436:214–220. [PubMed: 15951802]
27. Chen CZ, Li L, Lodish HF, Bartel DP. MicroRNAs modulate hematopoietic lineage differentiation. Science. 2004; 303:83–86. [PubMed: 14657504]
28. Smirnova L, et al. Regulation of miRNA expression during neural cell specification. The European Journal of Neuroscience. 2005; 21:1469–1477. [PubMed: 15845075]
29. Panganiban G, Rubenstein JL. Developmental functions of the Distal-less/Dlx homeobox genes. Development. 2002; 129:4371–4386. [PubMed: 12223397]
30. Nyfeler Y, et al. Jagged1 signals in the postnatal subventricular zone are required for neural stem cell self-renewal. The EMBO Journal. 2005; 24:3504–3515. [PubMed: 16163386]
31. Finzsch M, Stolt CC, Lommes P, Wegner M. Sox9 and Sox10 influence survival and migration of oligodendrocyte precursors in the spinal cord by regulating PDGF receptor {alpha} expression. Development. 2008; 135:637–646. [PubMed: 18184726]
32. Stolt CC, et al. The Sox9 transcription factor determines glial fate choice in the developing spinal cord. Genes & Development. 2003; 17:1677–1689. [PubMed: 12842915]
33. Nowak JA, Polak L, Pasolli HA, Fuchs E. Hair follicle stem cells are specified and function in early skin morphogenesis. Cell Stem Cell. 2008; 3:33–43. [PubMed: 18593557]
34. Bastide P, et al. Sox9 regulates cell proliferation and is required for Paneth cell differentiation in the intestinal epithelium. The Journal of Cell Biology. 2007; 178:635–648. [PubMed: 17698607]
35. Vidal VP, et al. Sox9 is essential for outer root sheath differentiation and the formation of the hair stem cell compartment. Curr Biol. 2005; 15:1340–1351. [PubMed: 16085486]
36. Krichevsky AM, King KS, Donahue CP, Khrapko K, Kosik KS. A microRNA array reveals extensive regulation of microRNAs during brain development. RNA. 2003; 9:1274–1281. [PubMed: 13130141]
37. Bartel DP, Chen CZ. Micromanagers of gene expression: the potentially widespread influence of metazoan microRNAs. Nat Rev Genet. 2004; 5:396–400. [PubMed: 15143321]
38. Ballas N, Grunseich C, Lu DD, Speh JC, Mandel G. REST and its corepressors mediate plasticity of neuronal gene chromatin throughout neurogenesis. Cell. 2005; 121:645–657. [PubMed: 15907476]
39. Singh SK, Kagalwala MN, Parker-Thornburg J, Adams H, Majumder S. REST maintains self-renewal and pluripotency of embryonic stem cells. Nature. 2008; 453:223–227. [PubMed: 18362916]
40. Choi PS, et al. Members of the miRNA-200 family regulate olfactory neurogenesis. Neuron. 2008; 57:41–55. [PubMed: 18184563]
41. Silber J, et al. miR-124 and miR-137 inhibit proliferation of glioblastoma multiforme cells and induce differentiation of brain tumor stem cells. BMC Med. 2008; 6:14. [PubMed: 18577219]
42. Lim DA, et al. Noggin antagonizes BMP signaling to create a niche for adult neurogenesis. Neuron. 2000; 28:713–726. [PubMed: 11163261]

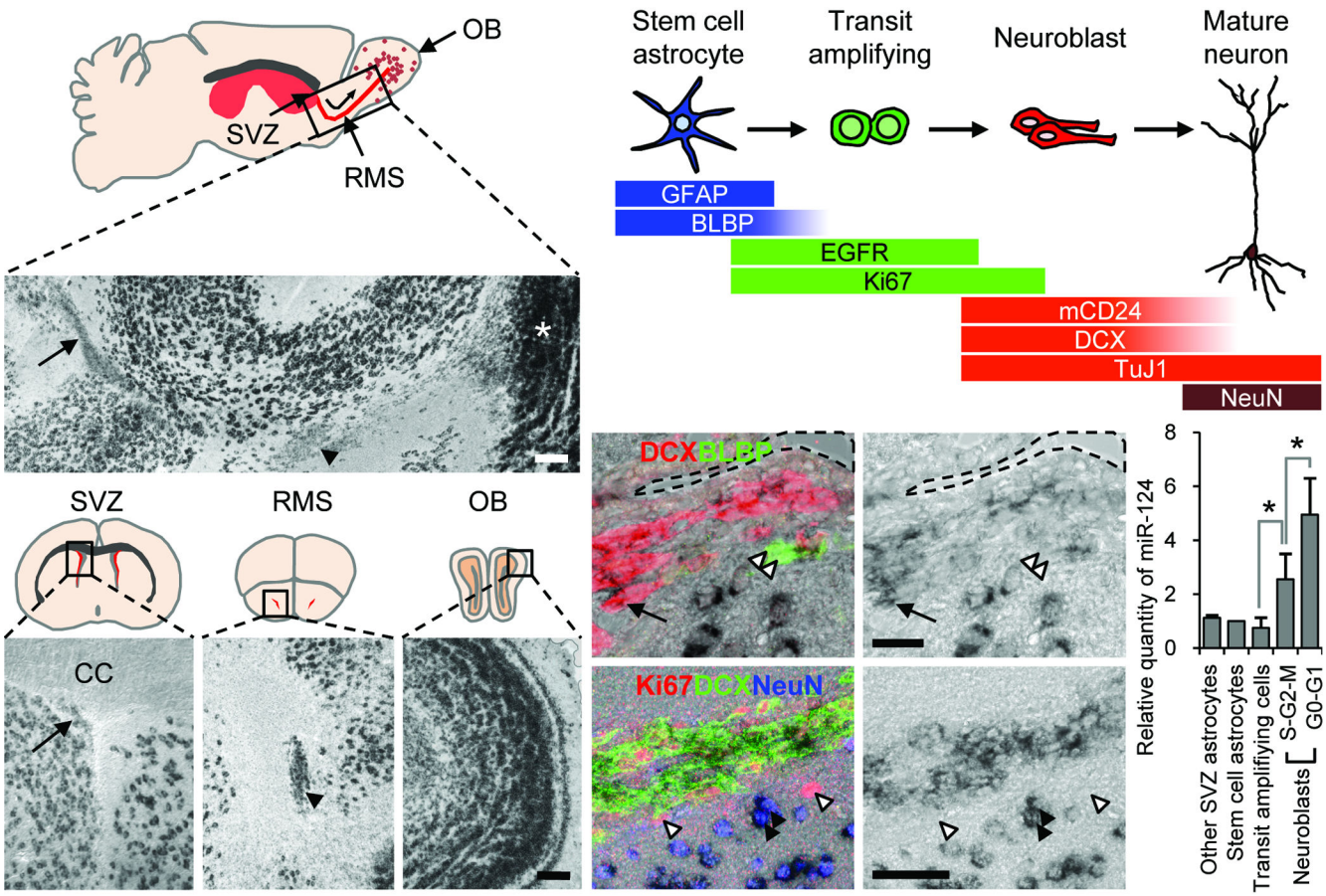

Figure 1. miR-124 expression in the adult SVZ niche

(**a**–**e**) *In situ* hybridization of miR-124 in the adult mouse brain. (**a**) Sagittal schema showing SVZ (red), which extends along the entire lateral ventricle. Image in (**b**) corresponds to area in box in (**a**). miR-124 is expressed at low levels in the SVZ (arrow) and RMS (arrowhead) and is up-regulated in the olfactory bulb (OB, asterisk). Other labeled cells are differentiated neurons (see Supplementary Fig. 1a). (**c**–**e**) miR-124 signal in coronal sections corresponding to areas shown in boxes in SVZ (**c**, arrow), RMS (**d**, arrowhead) and OB (**e**). miR-124 is not detected in the corpus callosum (**c**, CC) or other white matter fiber tracts. Scale bar, 100μm. (**f**) Schema showing the SVZ lineage and markers expressed at each stage. (**g**, **h**) *In situ* hybridization for miR-124 combined with immunostaining in SVZ coronal sections. CC is at top and striatum is at bottom. Right panels show in situ signal alone. (**g**) miR-124 is expressed in DCX^+ neuroblasts (red, arrow) but not in $BLBP^+$ astrocytes (green, white arrowheads). Dashed lines outline the lateral ventricle. (**h**) miR-124 is expressed in DCX^+ neuroblasts (green) and in mature $NeuN^+$ neurons (blue, black arrowheads) but is not detected in $Ki67^+DCX^-$ transit amplifying cells (red, white arrowheads). Scale bar, 20μm. (**i**) Quantitative RT-PCR for miR-124 on FACS purified SVZ populations. Data represent mean ± s.e.m. normalized to 5S rRNA from five independent experiments. Asterisks, $p<0.05$, two-tailed paired Students-*t* test.

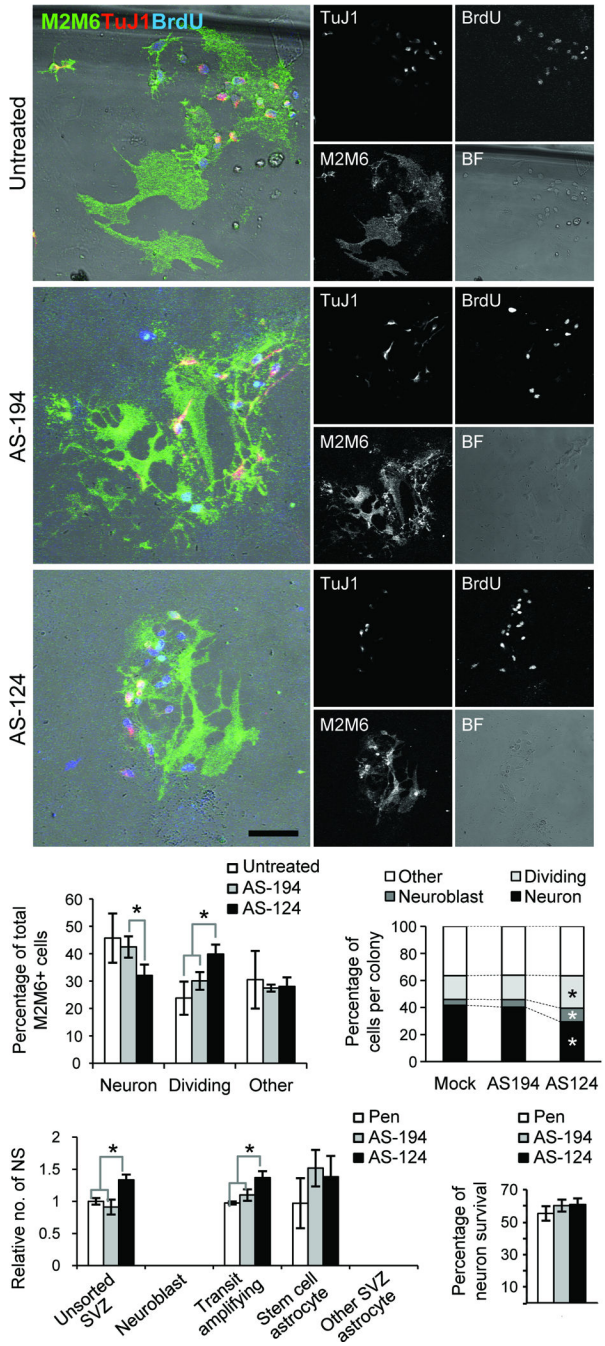

Figure 2. Knockdown of miR-124 *in vitro*

(**a**–**c**) Representative micrographs of colonies from SVZ stem cells co-cultured on rat astrocyte monolayers in the presence of penetratin (pen)-conjugated antisense 2'OMe-RNAs against miR-124 (AS-124) or miR-194 (AS-194). M2/M6 (green) distinguishes mouse cells on immunonegative rat cells. More $BrdU^+$ cells (blue) and fewer neurons (TuJ1, red) are present in AS-124 treated cultures. BF, bright field. Scale bar, 50 μm. (**d**) Quantification of total neurons ($TuJ1^+BrdU^-$), dividing cells ($BrdU^+$) and other cells ($TuJ1^-BrdU^-$). (**e**) Colony composition of neurons ($TuJ1^+BrdU^-$), neuroblasts ($TuJ1^+BrdU^+$), dividing cells

(BrdU$^+$) and other cells (TuJ1$^-$BrdU$^-$) within individual colonies. AS-124 treatment decreases the proportion of neurons (black) derived from single SVZ stem cells by maintaining them as dividing neuroblasts (dark gray) and transit amplifying cells (light gray). (**f**) Quantification of neurosphere (NS) formation of unsorted and FACS purified cells. Histogram shows ratio to untreated culture. (**g**) Quantification of survival of FACS purified neuroblasts. All data represent mean ± s.e.m. from at least three independent experiments. Asterisks, $p<0.05$, two-tailed paired Students-*t* test.

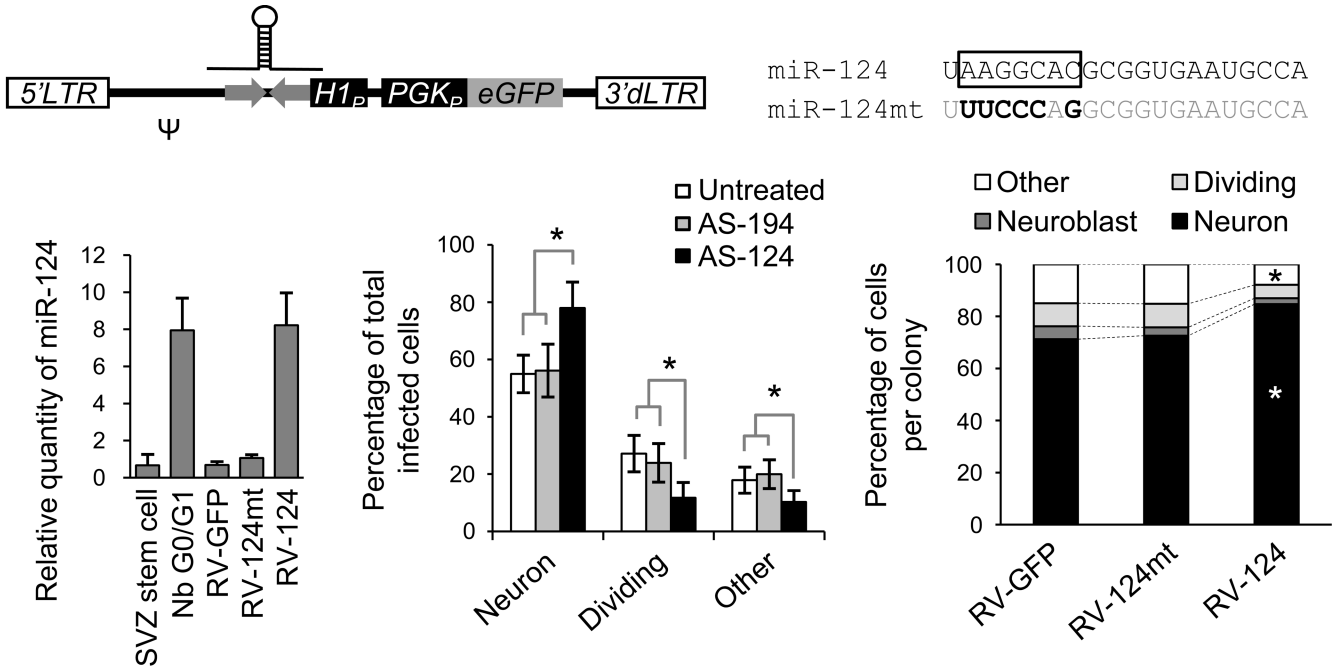

Figure 3. Ectopic expression of miR-124 *in vitro*

(**a**) Schema shows the retroviral construct for miR-124 over-expression. The mouse *mir-124–3* genomic locus (hairpin) with ~125 bp flanking sequences was cloned into the murine stem cell virus (MSCV) backbone under the control of the *H1* promoter. The expression of enhanced GFP was driven by a second promoter (*PGK* promoter) placed in the opposite orientation to the miRNA expression cassette. (**b**) Sequence of mutated miR-124 in the retroviral construct (RV-124mt). Six nucleotides (bold) of the 5' seed region (box) were mutated. (**c**) Quantitative RT-PCR of miR-124 levels induced by retroviral infection in neurospheres. Neurospheres transduced by RV-124 ectopically express miR-124 to the physiological levels present in purified neuroblasts (mCD24 population). (**d**) Quantification of GFP^+ neurons ($TuJ1^+BrdU^-$) dividing cells ($BrdU^+$) and other cells ($TuJ1^-BrdU^-$) after miR-124 over-expression. (**e**) Colony composition of neurons ($TuJ1^+BrdU^-$, black), neuroblasts ($TuJ1^+BrdU^+$, dark gray), dividing cells ($BrdU^+$, light gray) and other cells ($TuJ1^-BrdU^-$, white) within individual colonies after RV-124 over-expression. All data represent mean ± s.e.m. from six independent experiments. Asterisks, $p<0.05$, two-tailed paired Students-*t* test.

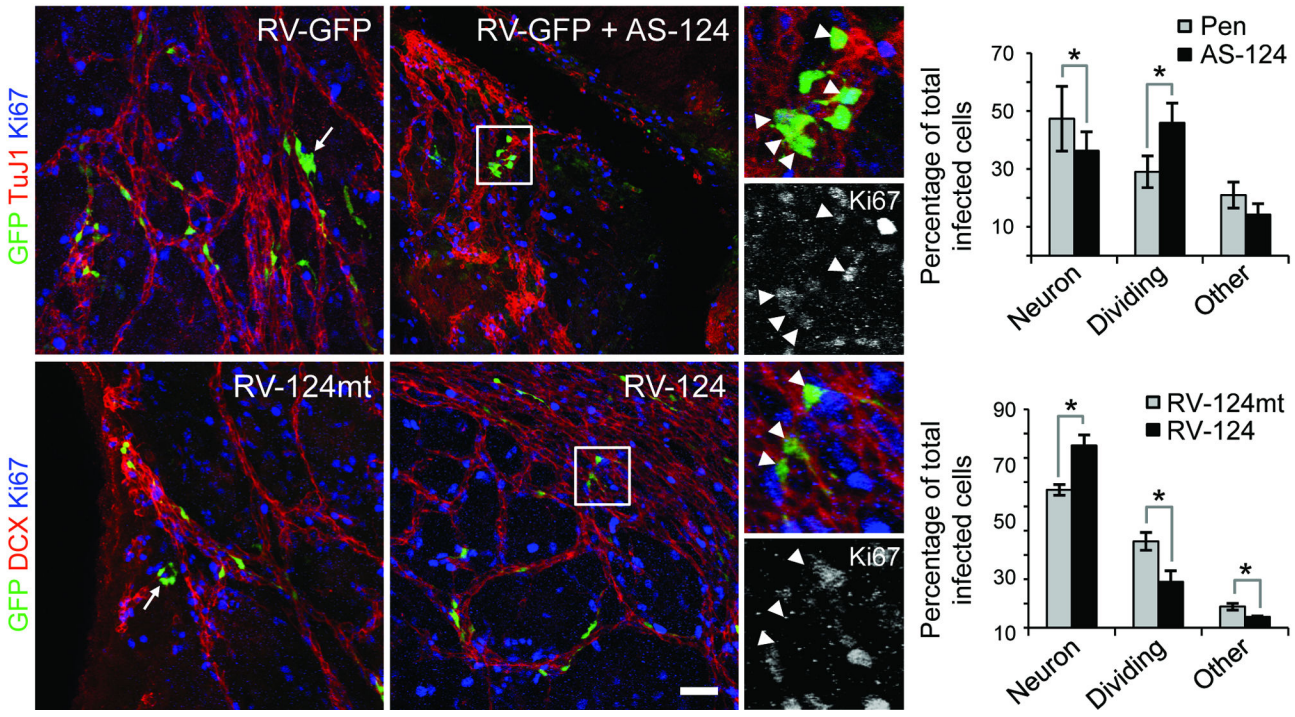

Figure 4. miR-124 over-expression and knockdown *in vivo*

(**a**–**c**,**e**–**g**) Representative micrographs of SVZ whole mount preparations three days after retrovirus infection. GFP$^+$ dividing cells (arrows) and migratory neuroblasts (in chains, TuJ1$^+$ or DCX$^+$, red) were present after RV-GFP (**a**), RV-GFP +AS-124 (**b**), RV-124mt (**e**) and RV-124 (**f**) infection. (**c**,**g**) are higher magnification view of boxes in **b** and **f**, respectively. Lower panels show split channel of Ki67 immunostaining. AS-124 maintains SVZ precursors as clusters of dividing cells (**c**, arrowheads) whereas RV-124 induces cell cycle exit and neuronal differentiation (**g**, arrowheads indicate post-mitotic migrating neurons). Scale bar, 50 μm. (**d, h**) Quantification of total neurons (TuJ$^+$Ki67$^-$ or DCX$^+$Ki67$^-$), dividing cells (Ki67$^+$) and other cells (Ki67$^-$DCX$^-$) derived from infected SVZ precursors after miR-124 knockdown (**d**) and RV-124 over-expression (**h**). Data represent mean ± s.e.m from six whole mounts. Asterisks, $p<0.05$, two-tailed paired Students *t*-test. A total of n=1260 (RV-GFP with saline), n=492 (RV-GFP with penetratin-only), n=477 (RV-GFP with AS-124), n=895 (RV-124), and n=938 (RV-124mt) retrovirally transduced cells were counted.

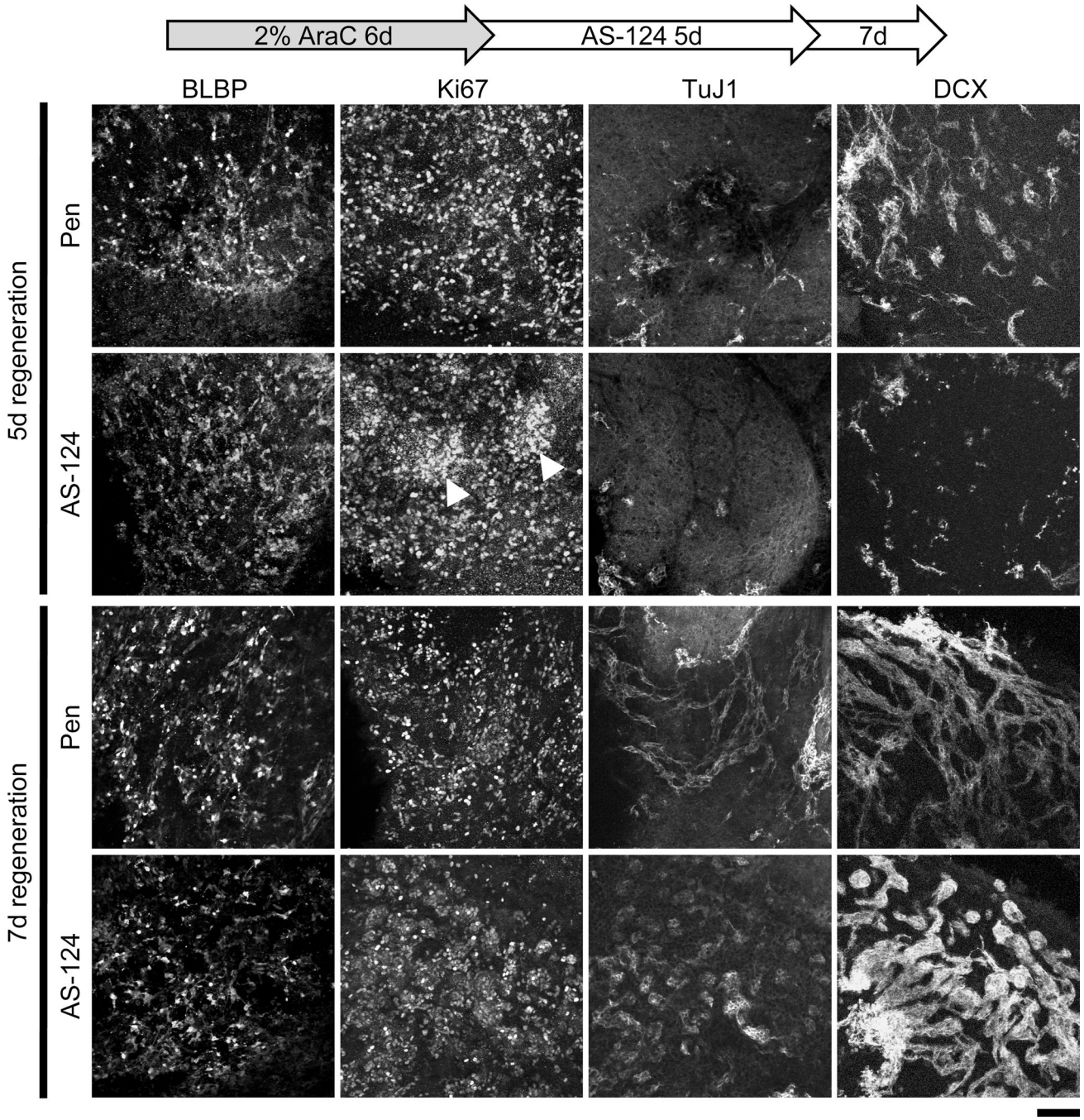

Figure 5. miR-124 knockdown delays SVZ regeneration

(**a**) Timeline of experiments. Ara-C filled mini-osmotic pumps were implanted for 6 days and replaced by AS-124 or penetratin-only filled pumps for an additional 5 or 7 days. (**b**–**q**) SVZ whole mount preparations after five (**b**–**i**) or seven (**j**–**q**) days of regeneration immunostained for BLBP (**b**,**f**,**j**,**n**), Ki67 (**c**,**g**,**k**,**o**), TuJ1 (**d**,**h**,**l**,**p**) and DCX (**e**,**i**,**m**,**q**). At 5 days, more dividing cells and small hyperplasias (**g**, arrowheads) and very few neuroblasts (**h**,**i**) are present in AS-124 treated brains. At seven days, a large number of $TuJ1^+$ and DCX^+ neuroblasts suddenly appear (**p**,**q**).

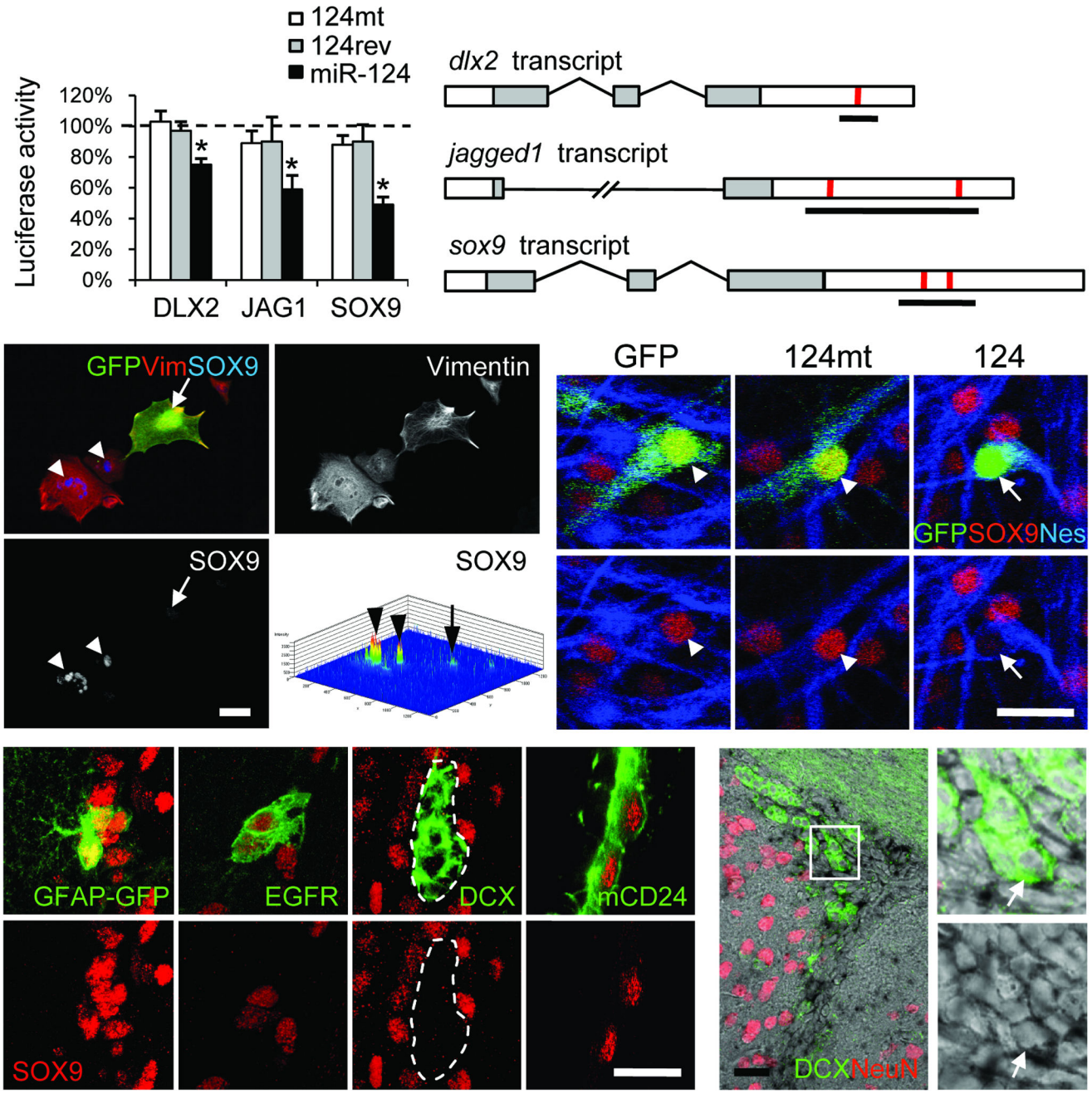

Figure 6. Sox9 is a miR-124 target

(**a**) Luciferase reporter assays for DLX2, JAG1 and SOX9, three miR-124 targets. Histogram showing ratio of Renilla to Firefly luciferase activity normalized to empty vector transfected cells (baseline). Data represent mean ± 2x s.e.m. from six independent experiments. Asterisks, $p<0.01$, two-tailed paired Student-*t* test. (**b**) Schema of *dlx-2*, *jagged1* and *sox9* transcripts and miR-124 target sites (red). Lines underneath depict region of 3'UTR cloned into luciferase reporter vectors. (**c**–**f**) miR-124 over-expression in neonatal astrocytes. Immunostaining for Sox9 (blue, **c**,**e**), Vimentin (red, **c**,**d**) and GFP (green, **c**). Sox9 protein is down-regulated by miR-124 over-expression (**c**, **e,** arrow) as compared to

untransfected cells (**c**–**e,** arrowheads), shown in corresponding fluorescence intensity plot (**f**, red is bright, blue is dim). (**g**–**i**) miR-124 over-expression in undifferentiated adult SVZ adherent cultures. Immunostaining for Sox9 (red), Nestin (blue) and GFP (green). Sox9 protein is down-regulated by miR-124 over-expression (**i**, arrows) but not by controls (**g**,**h,** arrowheads). (**j**–**m**) Sox9 immunostaining in coronal sections of adult mouse SVZ. Sox9 (red, upper and lower panels) is expressed by GFP^+ SVZ astrocytes in *hGFAP-GFP* mice (**j**), by a subset of $EGFR^+$ transit amplifying cells (**k**, green) and $mCD24^+$ ependymal cells (**m**, green). DCX^+ neuroblasts (**l**, green, outlined) lack Sox9 protein. (**n**–**p**) *In situ* hybridization of *Sox9* (black signal) combined with immunostaining for DCX (green) and NeuN (red). (**o**,**p**) High magnification view of box in (**n**) showing *sox9* mRNA (arrow, **p**) in a DCX^+ neuroblast (arrow, **o**). Scale bars, 20 μm.

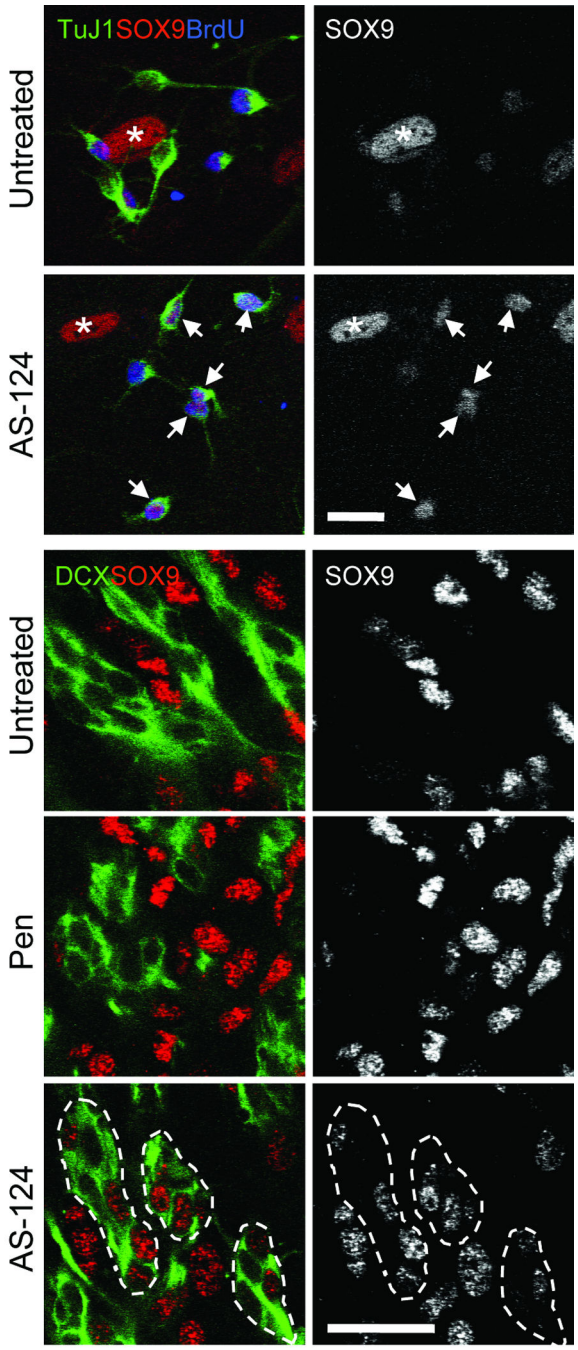

Figure 7. Effect of miR-124 knockdown on Sox9 protein levels

(**a**,**b**) Immunostaining of TuJ1 (green), Sox9 (red) and BrdU (blue) in 5 DIV co-cultures. Right panels show Sox9 channel. In untreated cultures, $BrdU^+$ dividing neuroblasts express low or undetectable levels of Sox9 protein (**a**). AS-124 treatment up-regulates SOX9 protein expression in dividing neuroblasts (**b**, arrows). Note that rat astrocyte monolayer underneath also expresses Sox9 (**a**,**b**, asterisks). (**c**–**e**) Immunostaining of DCX (green) and Sox9 (red) in coronal sections of the adult mouse brain. Right panels show Sox9 channel in untreated, penetratin-only (pen) and AS-124 infused brain. After 6 days of AS-124 infusion, Sox9

protein was ectopically expressed by migrating DCX^+ neuroblasts in the RMS (**e**, outlined by dashed lines). Scale bars, 20 μm.

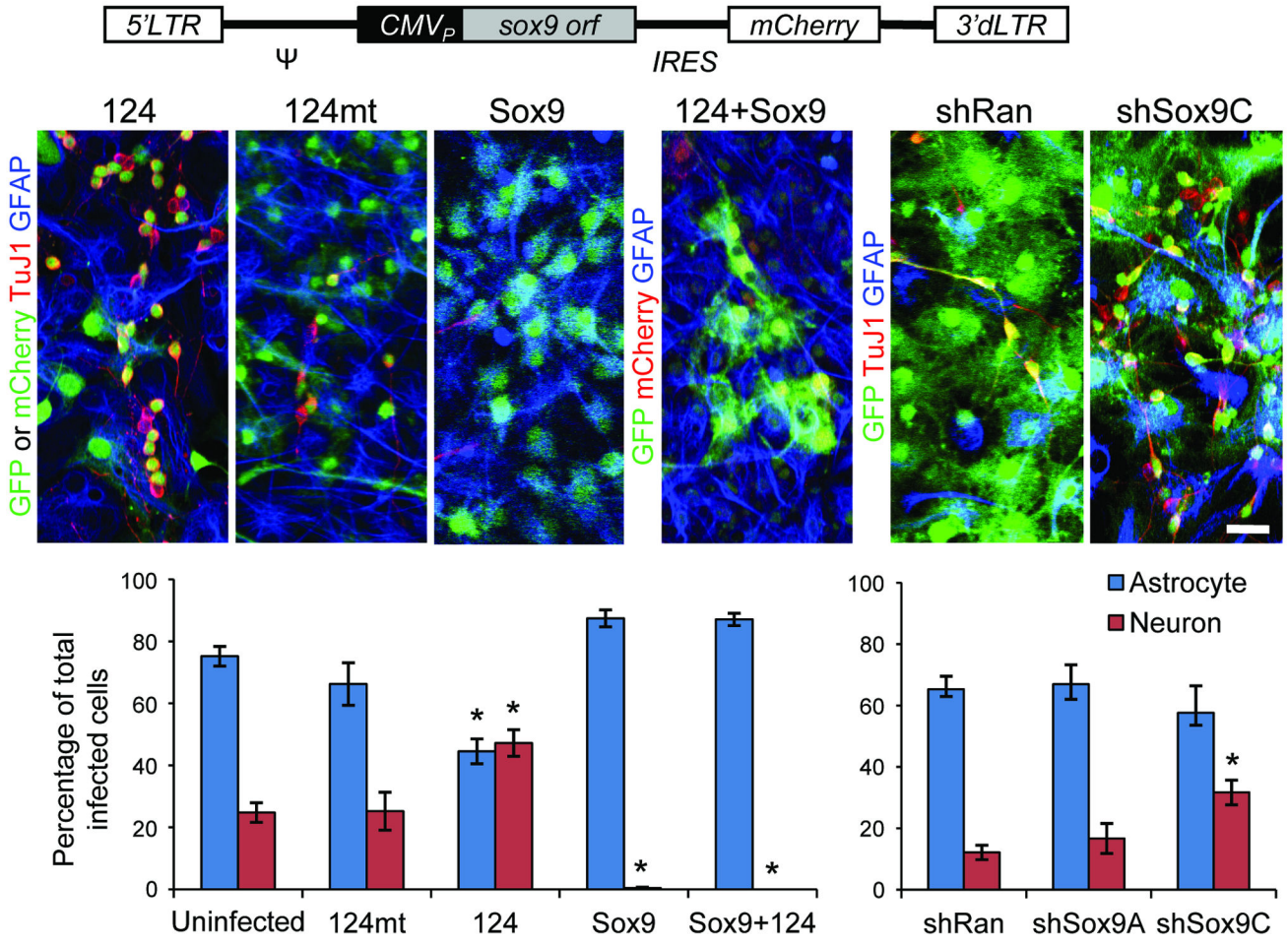

Figure 8. Sox9 knockdown induces neuronal differentiation

(**a**) Schema of the Sox9 retroviral construct (RV-Sox9). *Sox9* open reading frame (ORF) and the reporter gene (*mCherry*) are under control of the *CMV* promoter and are transcribed as bicistronic transcripts. The internal ribosomal entry sites (IRES) allow the expression of mCherry. (**b**–**g**) Representative micrographs of retrovirally transduced SVZ adherent cultures after 7 days of differentiation following EGF withdrawal. Immunostaining for GFAP (blue), TuJ1 (red) and reporter genes (GFP or mCherry, green, except for **e**, mCherry in red). RV-124 induces neuron production at the expense of astrocyte formation (**b**) as compared to RV-124 mt controls (**c**). In contrast, Sox9 over-expression eliminates neurogenesis and maintains infected cells as $GFAP^+$ astrocytes (**d**). Sox9 lacking a 3'UTR dominates the gliogenesis phenotype and is not rescued by miR-124 over-expression (**e**). Sox9 knockdown by RV-shSox9-C (**g**) increases neuronal differentiation as compared to controls (**f**) and resembles the phenotype of RV-124 transduced cells. Scale bar, 20 μm. (**h**,**i**) Quantification of astrocytes ($GFAP^+$) and neurons ($TuJ1^+$) present after retroviral infection. Data represent mean ± s.e.m. from at least three independent experiments. Asterisks, $p<0.01$, two-tailed paired Students-t test. The percentages of both astrocytes and neurons in RV-124, RV-Sox9, and RV-124/RV-Sox9 are statistically significant as compared to the

uninfected and RV-124mt controls (**h**). The percentage of neurons in RV-shSox9-C is significantly higher as compared to RV-shRan and RV-shSox9-A (**i**).